



An empirical scaling law for acquisition of thermoremanent magnetization

Gunther Kletetschka^{a,b,c,*}, M.H. Acuna^c, Tomas Kohout^{b,d},
Peter J. Wasilewski^c, John E.P. Connerney^c

^aDepartment of Physics, Catholic University of America, Washington DC, USA

^bInstitute of Geology, Academy of Sciences, Prague, Czech Republic

^cNASA/Goddard Space Flight Center, Code 691 Greenbelt, MD 20771, USA

^dDepartment of Applied Geophysics, Faculty of Natural Sciences, Charles University, Prague, Czech Republic

Received 3 March 2004; received in revised form 2 August 2004; accepted 2 August 2004

Available online 13 September 2004

Editor: R.D. van der Hilst

Abstract

We describe a universal linear relationship between the acquisition magnetic field, B , and thermoremanent magnetization $M_{tr}(T_r)$ measured at room temperature T_r . The efficiency $\varepsilon(T_r)$ of a remanent magnetization (REM) is the ratio of the natural remanent magnetization $M_{nr}(T_r)$ to the saturation remanence $J_{sr}(T_r)$. We report a power law relationship with exponent related to $J_s(T_r)$ and unit slope indicating a linear relationship. Thus $\log \varepsilon(T_r)$ of $M_{tr}(T_r)$ in equidimensional-shaped magnetic minerals of contrasting saturation magnetization $J_s(T_r)$ plots linearly with the logarithm of the applied magnetic field B along separate grain-size-independent straight lines with nearly unit slope and offsets related to $J_s(T_r)$. This empirical relationship is well suited for paleofield-intensity estimation, predicts strong magnetization of hematite and pyrrhotite in weak fields, and can be used as an assessment tool for observed remanence in planetary and meteoritic objects.

© 2004 Elsevier B.V. All rights reserved.

Keywords: thermoremanent magnetism; efficiency of remanent magnetism; saturation magnetism; paleointensity; magnetic mineralogy; Néel theory; grain size

1. Introduction

The intensity of the remanent magnetization acquired by rocks has been studied sporadically by normalization [1–6] and is critically dependent on the unknown strength of the ambient magnetic field and the unknown magnetic mineral composition. Anomalous

* Corresponding author. Tel.: +1 301 286 3804; fax: +1 301 286 0212.

E-mail address: gunther.kletetschka@gsfc.nasa.gov
(G. Kletetschka).

intensities have been reported in hematite and titanohematite [7–9] with intensities close to saturation. There is just one distinct mechanism that allows homogenous and efficient magnetizations in natural conditions (e.g. within the Earth's crust). This is when magnetic grains record magnetization at the mineral- and size-dependent blocking temperatures (T_b) below which the magnetic remanence is stable in time. Stacey [10] pointed out in his theory of multidomain TRM, since the demagnetizing energy falls off more slowly with temperature than any other, the condition under which TRM is first acquired is simply the minimization of the internal field. This guarantees that at least at this temperature the TRM is related only to the magneto-static energy and the demagnetizing energy. In the Néel theory (recognized as incomplete since it fails to describe many aspects of pTRM behavior [11]) of TRM [12] in MD grains, blocking occurs at T_b when barriers to wall motion, described by magnetic coercivity, grow high enough to pin domain walls against the demagnetizing field. For SD grains $M_{tr}(T_r)$ is a frozen-in high temperature equilibrium distribution achieved by thermally excited transitions among the different magnetic states. Transitions cease below the T_b , because in the course of cooling the energy barriers between different magnetization states grow larger than the available thermal energy. For both SD and MD states the resulting magnetization, composed of many magnetic moments, is in the direction of and proportional to the applied magnetic field B . Efficiency $\varepsilon(T_r)$ of $M_{tr}(T_r)$ of SD grains of saturation remanence $J_{sr}(T_r)$, volume V and saturation magnetization $J_s(T_b)$ is [13]:

$$\varepsilon(T_r) = \frac{M_{tr}(T_r)}{J_{sr}(T_r)} = \tanh\left(\frac{\mu_0 V J_s(T_b) B}{k T_b}\right), \quad (1)$$

with $\mu_0 = 4\pi \times 10^{-7}$, and $k = 1.38 \times 10^{-23}$ J/K. For empirical experiments we approximate [14]: $\frac{\mu_0 V J_s(T_b) B_c(T_b)}{k T_b} \approx 50$, where $B_c(T_b)$ is a critical field for rotations in the absence of thermal energy (micro-coercivity). Therefore from Eq. (1) we can derive for small fields ($\varepsilon \ll 1$):

$$\varepsilon(T_r) = \frac{50B}{B_c(T_b)} \quad (2)$$

In most fine-grained magnetic material, a typical efficiency $\varepsilon(T_r)$ of thermoremanent magnetization

$M_{tr}(T_r)$ acquired in the geomagnetic field is about 1% [1,3,15,16]. This small efficiency is consistent with the $M_{tr}(T_r)$ acquisition curves for magnetite [17–19] with grain sizes covering the range from the single domain (SD) to multidomain (MD) magnetic states. However, $M_{tr}(T_r)$ experiments with hematite [7,14,20,21] show $\varepsilon > 10\%$.

2. Material and method

Consequently to reconcile this contrast we performed a series of magnetic M_{tr} acquisitions using six distinct magnetic materials (Table 1): iron (Fe), iron–nickel (FeNi), magnetite (Fe_3O_4), hematite ($\alpha\text{-Fe}_2\text{O}_3$), and resistance wires MWS-294R and ALLOY52. All samples, except the wires and iron nickel (polycrystalline), were single crystals about 1 mm in size. Squareness ratios (Table 1) span a large range of values (0.001–0.9). The iron sample (Iron (IA) coarse Octahedrite) was characterized by scanning electron microscope (SEM) microprobe measurements (only Fe present) and saturation magnetization ($J_s = 1700$ kA/m). The iron–nickel sample is an industrial product with about 50% nickel, based on SEM microprobe measurements. The magnetite sample 90LP12 is a non-titanium magnetite obtained from

Table 1
Squareness ratios J_{sr}/J_s for samples used in Figs. 1 and 3

Sample	J_{sr}/J_s
Iron1	9.69E–03
Iron2	8.93E–03
Iron3	9.01E–03
Iron4	9.59E–03
Iron–nickel1	4.59E–03
Iron–nickel2	4.53E–03
Iron–nickel3	1.30E–03
Magnetite1	3.42E–02
Magnetite2	2.50E–02
Magnetite3	1.13E–02
Pyrrhotite	2.50E–01
Hematite1	8.54E–01
Hematite2	8.78E–01
Hematite3	9.00E–01
1/5 MWS-294R	1.16E–02
1/14 MWS-294R	1.20E–02
1/5 ALLOY52	3.68E–03
1/14 ALLOY52	8.22E–03

Pyrrhotite data are based on previous study by Dekkers [24].

Prof. John Valley, University of Wisconsin. The composition of this sample was characterized [20] by X-ray, Curie temperature, Verwey transition, and saturation magnetization. The hematite sample L2 is a coarse-grained variety from the Fire Lake mine in Central Labrador, Canada. Its composition was characterized [20–22] by X-ray, Curie temperature, Morin transition and saturation magnetization. Wires were obtained from MWS Wire Industries. Wires MWS-294R and ALLOY52 have chemical composition of 29% Ni, 17% Co, 54% Fe and 50.5% Ni, 49.5% Fe, respectively.

Each sample was brought to 800 °C and held there for 30 min in a residual magnetic field less than 10^{-8} T and ambient atmosphere. Samples were subsequently cooled to room temperature T_r in controlled (5% of its nominal value) homogenous magnetic fields (5×10^{-7} to 5×10^{-3} T). We detected an effect of isothermal magnetic acquisition (IRM) for $M_{tr}(T_r)$ acquired below the minimum value of 5×10^{-7} T during the sample transport in the non-shielded laboratory (5×10^{-5} T).

Equidimensional-shape material samples were represented by three to four specimens each (Table 1).

For wire samples, specimens of two different length vs. diameter ratios (1/5 and 1/14) were used.

The magnitude of $M_{tr}(T_r)$ was measured by a superconducting rock magnetometer (SRM) at a temperature of 300 K and ambient atmosphere. Subsequent magnetic hysteresis loop measurements of each sample provided estimates of saturation magnetization, $J_s(T_r)$, and saturation isothermal remanent magnetization, $J_{sr}(T_r)$. The $J_s(T_r)$ values measured before and after the $M_{tr}(T_r)$ acquisitions provided a magnetic proxy for unwanted chemical changes that may have occurred during the heating. However, owing to the large grain size of our samples (~1 mm), we did not detect any chemical changes during the thermal treatments.

3. Results and discussion

Fig. 1 shows the field B required to reach efficiency $\varepsilon(T_r)$ of the $M_{tr}(T_r)$ acquisition for equidimensional samples and a literature sample of acicular magnetite [23] in which the crystals are highly elongated parallel to the applied field. In our

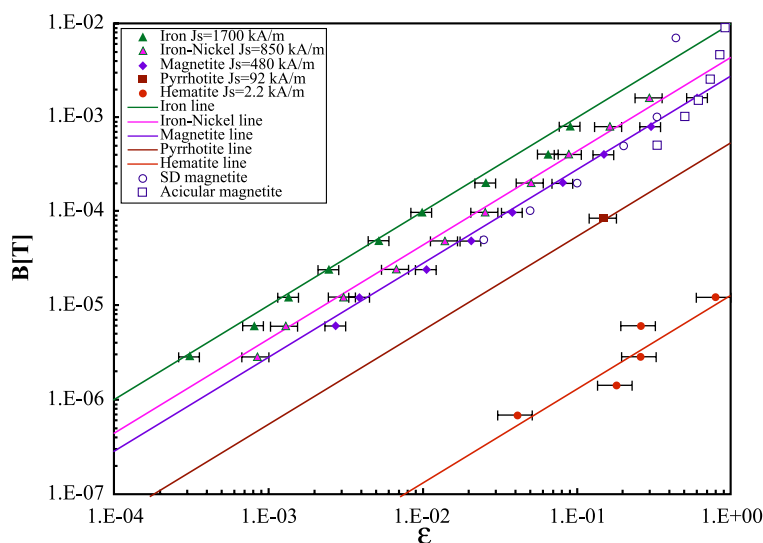


Fig. 1. Intensities of the ambient magnetic field B [Tesla] against thermoremanent efficiencies ε of hematite (Fe_2O_3), magnetite (Fe_3O_4), iron–nickel alloy (FeNi) and iron (Fe). The pyrrhotite data (Fe_7S_8) are from Dekkers [24]. Straight lines are drawn according to $B = a\varepsilon J_s$, where a is a dimensionless constant equal to 0.0046 (see Fig. 3a) at 300 K, and $J = \mu_0 J_s$ where μ_0 is permeability of vacuum and J_s is saturation magnetization at 300 K. Magnetization efficiency ε is defined as $\varepsilon = M_{tr}/J_{sr}$, the ratio of thermoremanence to saturation remanence. Single domain (SD) and acicular (elongated crystal parallel to the applied field) magnetite data are redrawn from Dunlop and Argyle [23] and Dunlop and West [34], respectively.

data, we excluded values near and at saturation where the simple power law breaks down (see Fig. 2). We also added literature data for pyrrhotite [24] for completeness. Each mineral is restricted to its own line with the unit slope in the $\log B$ – $\log \varepsilon$ space. In general, the larger the $J_s(T_r)$ (see legend) the larger the field B required to achieve a predefined efficiency level ε .

We propose the following hypothesis. An increase of the minerals' $J_s(T_r)$ is equivalent to similar increase in opposing demagnetizing field $H_d(T_r)$ [14,20,21,25] as well as critical fields B requiring material to reach the saturation magnetization at T_b . The demagnetizing field at saturation relates to $B_c(T_b)$ above which the energy minima become unstable causing the magnetic moment to irreversibly rotate in an absence of thermal fluctuations. Low $J_s(T_r)$ value is associated with low value of both $B_c(T_b)$ and H_d and leads to a large critical SD size and large magnetic domain wall spacing while large $J_s(T_r)$ implies large $B_c(T_b)$ (or H_d) causing a fine scale of the individual domains. Other effects, like magnetostriction, anisotropy and exchange constants, may also cause changes in the overall magnetic domain size.

Our data in Fig. 1 are representative of multi-domain (MD) magnetic materials (1 mm grain size). However, the $M_{tr}(T_r)$ varies with the grain size according to the domain type. For example, MD

magnetite has $M_{tr}(T_r)$ that increases with decreasing grain size [26]. Similar grain size dependence has been observed at saturation for $J_{sr}(T_r)$ [26] ($\varepsilon=1$). Thus efficiency $\varepsilon(T_r)$ of $M_{tr}(T_r)$ rather than just $M_{tr}(T_r)$ reduces the grain size dependence to a minimum, and a line separation in the $\log B$ – $\log \varepsilon$ plot can be used to identify the magnetic mineralogy in ideal circumstances.

The insensitivity of the $\log B$ – $\log \varepsilon(T_r)$ plot to various grain sizes is illustrated in Fig. 1 where the $M_{tr}(T_r)$ efficiency for SD magnetite [23] (literature data) correlates with our MD magnetites; this breaks down when mineral size becomes so small that it is near or in the superparamagnetic size range [23]. The grain size independence is also demonstrated in Fig. 2 where we plot literature data of various $M_{tr}(T_r)$ acquisitions of titanomagnetite with disparate magnetic domain states identified by the specific grain sizes [17–19]. Despite much stronger $M_{tr}(T_r)$ of fine vs. large magnetic grains, all sizes appear to have identical acquisitions when normalized by saturation remanence $J_{sr}(T_r)$.

When neglecting effects near saturation ($\varepsilon < 0.3$), this linear dependence predicts approximate maximum values of the magnetic field that can be recorded by a specific material (Fig. 1). Near the saturation the magnetization is not linear with the applied field (Fig. 2) owing to Eq. (1) when $\varepsilon \approx 1$. Thus the magnetic fields at which $\varepsilon = 1$ should be the

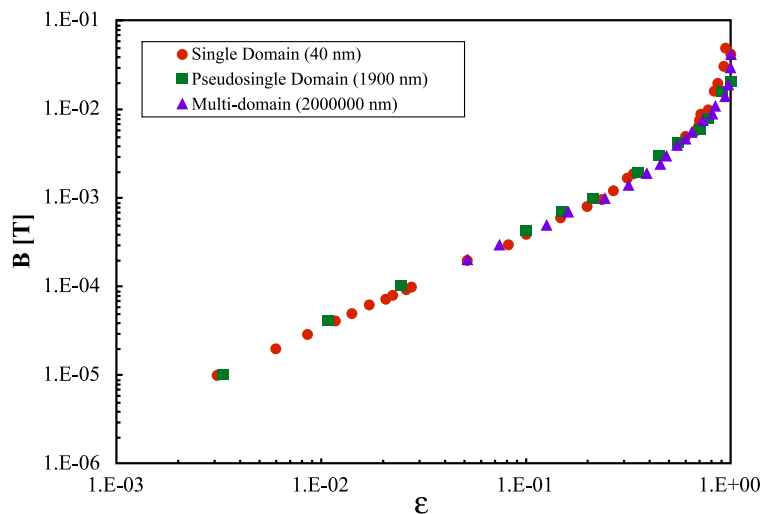


Fig. 2. Acquisition fields are plotted against thermoremanent efficiency for contrasting domain states of titanomagnetite. Data for multi-domain and pseudosingle domain mineral are from Tucker and O'Reilly [18]. Data for Single Domain minerals are from Özdemir and O'Reilly [19].

magnetic fields that define the values of intrinsic $B_c(T_b)$ for the specific mineral. Knowledge of $B_c(T_b)$ fields in principle can be used for dating of the magnetization according to known magnetization viscous decay curves [27,28]. $B_c \propto M_s$ for shape anisotropy, $B_c \propto (\lambda/M_s^n)$ for magnetoelastic anisotropy [29,30] (for $n>2$) and $B_c \propto (K/M_s^n)$ for crystalline anisotropy [31,32] (for $n>8$) where n is experimentally determined exponent. Both K and λ go to zero much faster than M_s , when approaching Curie temperature T_c . Energy minimum, related to magnetic ordering, is becoming shallower when approaching T_b due to thermal fluctuations [10]. Thus for the purpose of magnetic remanence blocking near T_c , we may consider only the shape anisotropy: $B_k \propto M_s$. The distribution of demagnetization field vectors (tensors in general [25]) relates to $B_c(T_b)$, the nature of the resulting $M_{tr}(T_r)$ and the $\varepsilon(T_r)$ dependencies. The $B_c(T_b)$ fields are small in minerals with low $J_s(T_r)$ causing them to reach saturation ($\varepsilon(T_r)=1$) in much lower applied fields B [14,20]. Larger $B_c(T_b)$ in minerals with large $J_s(T_r)$ creates larger resistance against acquisition of $M_{tr}(T_r)$ and requires larger magnetizing fields to achieve the saturation ($\varepsilon(T_r)=1$). For example, because magnetoelastic and crystalline constants go to zero much faster than M_s close to T_c hematite has low $B_c(T_b)$ (due to shape anisotropy) at the point at which TRM is acquired in contrast to its high B_c at room temperature caused by high magnetoelastic anisotropy.

In order to show the fundamental role of $J_s(T_r)$ in mineral specific $M_{tr}(T_r)$ acquisition we re-plot Fig. 1, multiplying the magnetic efficiency $\varepsilon(T_r)$ by $J(T_r)=\mu_0 J_s(T_r)$ (see Fig. 3a). This operation completely eliminates the effect of the demagnetizing field during the $M_{tr}(T_r)$ acquisition. Fig. 3a indicates that all of the mineral $M_{tr}(T_r)$ acquisitions can be well approximated (linear regression coefficient $R=0.97$) by a linear fit:

$$B = a(T)J(T)\varepsilon(T_r) \quad (3)$$

The value and statistical uncertainty of the $a(T)$ coefficient was estimated from the deviations of the data points from the least square fit. We find $a=(4.6\pm 0.3)\times 10^{-3}$ with 95% confidence level for $T=T_r=300$ K. The product $J_s(T_r)\varepsilon(T_r)$ is essentially the $M_{tr}(T_r)$ normalized by the squareness ratio $J_{sr}(T_r)/J_s(T_r)$ of the hysteresis loop. Thus, according to the

linear behavior (Fig. 3a), all magnetic materials should contribute to a planetary thermoremanent magnetic anomaly (e.g. intense magnetic anomalies detected on Mars [33]) with the same, squareness $J_{sr}(T_r)/J_s(T_r)$ -normalized, $M_{tr}(T_r)$ intensity. Because $J_s(T_r)$ eliminates the mineral dependence observed in Fig. 1 produced by variation in $B_c(T_b)$ in different minerals, we postulate that $B_c(T_b)=0.23 J_s(T_r)$ in Eq. (2) leading to empirically observed relationship (Eq. (3)). It is clear that the relationship (Eq. (3)) breaks down if the Curie temperature of the magnetic material gets near or below 300 K. With decreasing temperature, J_s increases and reaches a maximum at absolute zero temperature unless the material undergoes a phase transition (e.g. Verwey transition for magnetite). By extending the trend of the published $J_s(T)$ curves [25] into 0 K (ignoring any phase transitions), we get increase of J_s by a factor of 1.05 for iron, 1.00 for hematite, 1.10 for magnetite and 1.25 for pyrrhotite. This change of J_s values has negligible effect on Eq. (3). We still find near perfect linear relationship (Eq. (3)) where $a=(4.2\pm 0.3)\times 10^{-3}$ with 95% confidence level for $T=T_0=0$ K and $B_c(T_b)=0.21J(T_0)$. Using magnetic constants at absolute zero temperature, we eliminate the problem of Curie temperature and apply Eq. (3) for any magnetic material.

Because we propose that the microcoercivity $B_c(T_b)$ modifies the $M_{tr}(T_r)$ acquisition, the shape, magnetostriction and crystalline anisotropy of the carriers should have significant influence on the $M_{tr}(T_r)$ acquisition curves. For example, the length vs. diameter ratio of the carrier should reduce/increase the effect of $B_c(T_b)$ or demagnetizing field [25] for sample lengths parallel/perpendicular to the field and thus shift the $M_{tr}(T_r)$ acquisitions into lower/higher field intensities, respectively. In Fig. 1, we plot $M_{tr}(T_r)$ acquisition for acicular (elongated crystals parallel to the applied field) magnetite [34] with diameter to length ratio 1:7 that violates the equidimensionality assumption. Although the data are for magnetic fields near saturation of the magnetite, the demagnetizing field due to elongation causes these grains to acquire magnetization at lower fields than equidimensional magnetite grains. We verified this effect by measuring $M_{tr}(T_r)$ acquisition in industrial wires (MWS-294R and ALLOY52) with length to diameter ratios 1/5 and 1/14 (Fig. 3b)

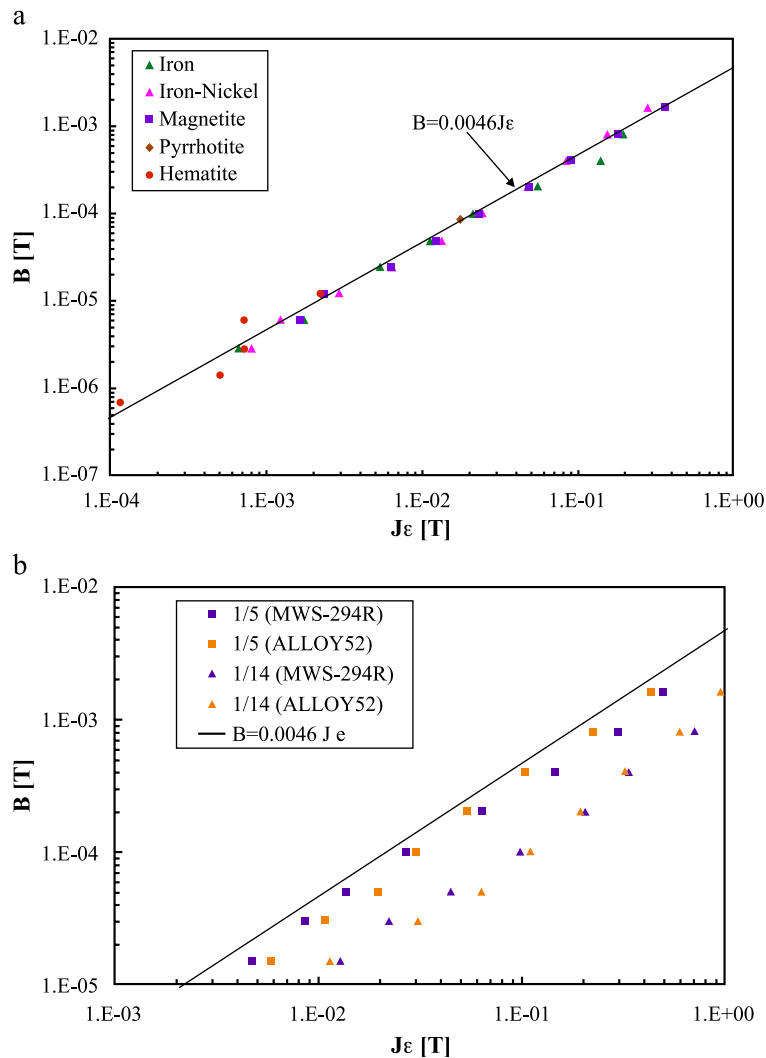


Fig. 3. Magnetic acquisition fields are plotted against $J\epsilon$, which is the saturation magnetization $J=\mu_0J_s$ multiplied by efficiency ϵ of various materials at 300 K. (a) Equidimensional grains of iron, iron–nickel, magnetite, pyrrhotite, and hematite define a straight line that is a result of a linear fit to all of the data. For J_s at 300 K, this fit has the form of $B=(4.6\pm 0.3)\times 10^{-3}J\epsilon$. The linear regression coefficients is $R=0.97$. (b) Effect of shape (non-equidimensional crystals) on thermoremanent acquisition fields for wire materials (MWS-294R and ALLOY52) with small (1/5) and large (1/14) predefined length to diameter ratios compared with the predicted acquisition (solid line) for equidimensional materials. Measurements were made with wires aligned parallel to the applied field.

where the longer wires, parallel to the field, clearly require lower fields to acquire the predicted intensity of magnetization.

The effect of placing wires perpendicular to the applied field should be equal and opposite to placing them parallel. Consequently for a large number of randomly oriented, elongated grains (such as is frequently the case in igneous rocks) ϵ

would follow the same relationships as for the single equidimensional grains used in this study. This makes the law far more applicable to those who study natural materials. However, this information would have to be accompanied by the caveat that, for the law to hold for multiple grains, the grains would have to be identical in size and composition (equal J_s , J_{sr} and M_{tr}).

It is important to emphasize that a substitution of ε to Eq. (3),

$$B = a(T_0)J_s(T_0) \frac{M_{tr}(T)}{J_{sr}(T)} \quad (4)$$

represents the first ever means to obtain a paleointensity determination using measurable quantities that does not involve the comparison of a TRM imparted in the lab with that acquired in nature. Practical considerations may pose a serious hindrance to it ever being used as such because the above equation would not be satisfied by bulk values and natural grains, capable of retaining a remanence over geological time, would be too small to be measured individually. Possible solutions involve isolating and amassing grains with sufficiently similar properties, decomposition of bulk values using FORC diagrams and so on to satisfy Eq. (4)'s requirements.

4. Conclusions

To summarize, we have found that for $\varepsilon \ll 1$ the magnetic thermoremanent acquisitions of minerals can be approximated by a relationship $B = a(T)J(T)\varepsilon(T_r)$ where a is a dimensionless constant $(4.6 \pm 0.3) \times 10^{-3}$ and $(4.2 \pm 0.3) \times 10^{-3}$ for T_r and T_0 , respectively, where $J(T) = \mu_0 J_s(T)$ (μ_0 is the vacuum permeability). $J(T_0)$ or $J(T_r)$ eliminates the dependence on micro-coercivity, suggesting that $B_c(T_b)$ in Eq. (2) can be approximated by $(2.1)J(T_0)$ or $(2.3)J(T_r)$, respectively. This relation (using $J(T_r)$) allows specification of $B_c(T_b)$ for the magnetic materials: B_c (iron)=490 mT, B_c (iron–nickel)=220 mT, B_c (magnetite)=140 mT, B_c (pyrrhotite)=27 mT, and B_c (hematite)=0.64 mT). These micro-coercivity fields can be reduced or increased further by variation in shape (Fig. 3b), crystalline anisotropy and magnetostriction.

Acknowledgements

This research was supported by the NASA sponsored Delaware Space Grant Consortium. We thank Norman F. Ness, Michael J. Jackson, Bruce M. Moskowitz, John C. Pearl, Lisa Tauxe and two

anonymous referees for valuable contributions. Suggestions made by other two non-anonymous referees, Mike Fuller and Andrew Biggen, significantly improved this manuscript.

References

- [1] P.J. Wasilewski, Magnetic and microstructural properties of some lodestones, *Physics of the Earth and Planetary Interiors* 15 (1977) 349–362.
- [2] P.J. Wasilewski, H.H. Thomas, M.A. Mayhew, The Moho as a magnetic boundary, *Geophysical Research Letters* 6 (1979) 541–544.
- [3] P.J. Wasilewski, Magnetization of small iron–nickel spheres, *Physics of the Earth and Planetary Interiors* 26 (1981) 149–161.
- [4] M. Fuller, S. Cisowski, M. Hart, R. Haston, E. Schmidtke, NRM:IRM(s) demagnetization plots; an aid to the interpretation of natural remanent magnetization, *Geophysical Research Letters* 15 (1988) 518–521.
- [5] P. Wasilewski, G. Kletetschka, Lodestone—nature's only permanent magnet, what it is and how it gets charged, *Geophysical Research Letters* 26 (15) (1999) 2275–2278.
- [6] P.J. Wasilewski, M.H. Acuna, G. Kletetschka, 433 Eros, problems with the meteorite magnetism record in attempting an asteroid match, *Meteoritics and Planetary Science* 37 (2002) 937–950.
- [7] G. Kletetschka, P.J. Wasilewski, P.T. Taylor, The role of hematite–ilmenite solid solution in the production of magnetic anomalies in ground and satellite based data, *Tectonophysics* 347 (1–3) (2002) 166–177.
- [8] P. Robinson, R.J. Harrison, S.A. McEnroe, R.B. Hargraves, Lamellar magnetism in the haematite–ilmenite series as an explanation for strong remanent magnetization, *Nature* 418 (2002) 517–520.
- [9] G. Kletetschka, N.F. Ness, P.J. Wasilewski, J.E.P. Connerney, M.H. Acuna, Possible mineral sources of magnetic anomalies on Mars, *The Leading Edge* 22 (8) (2003) 766–768.
- [10] F.D. Stacey, Thermoremanent magnetization (TRM) of multidomain grains in igneous rocks, *Philosophical Magazine* 3 (1958) 1391–1401.
- [11] V.V. Shcherbakova, V.P. Shcherbakov, F. Heider, Properties of partial thermoremanent magnetization in pseudosingle domain and multidomain magnetite grains, *Journal of Geophysical Research, [Solid Earth]* 105 (B1) (2000) 767–781.
- [12] L. Néel, Some theoretical aspects of rock magnetism, *Advances in Physics* 4 (1955) 191–243.
- [13] L. Néel, Théorie du traînage magnétique des ferromagnétiques en grains fins avec applications aux terres cuites, *Annales de Géophysique* 5 (1949) 99–136.
- [14] D.J. Dunlop, G. Kletetschka, Multidomain Hematite: a source of planetary magnetic anomalies? *Geophysical Research Letters* 28 (17) (2001) 3345–3348.
- [15] G. Kletetschka, P.T. Taylor, P.J. Wasilewski, H.G.M. Hill, The magnetic properties of aggregate polycrystalline diamond:

- Implication for carbonado petrogenesis, *Earth and Planetary Science Letters* 181 (3) (2000) 279–290.
- [16] S. Cisowski, M. Fuller, Lunar paleointensities via the IRMs normalization method and the early magnetic history of the moon, in: W.K. Hartmann, R.J. Phillips, G.J. Taylor (Eds.), *Origin of the Moon*, Lunar and Planetary Institute, Houston, 1986, pp. 411–424.
- [17] D.J. Dunlop, E.D. Waddington, Field-dependence of thermoremanent magnetization in igneous rocks, *Earth and Planetary Science Letters* 25 (1) (1975) 11–25.
- [18] P. Tucker, W. O'Reilly, The acquisition of thermoremanent magnetization by multidomain single-crystal titanomagnetite, *Geophysical Journal of the Royal Astronomical Society* 63 (1980) 21–36.
- [19] Ö. Özdemir, W. O'Reilly, An experimental study of the intensity and stability of thermoremanent magnetization acquired by synthetic monodomain titanomagnetite substituted by aluminium, *Geophysical Journal of the Royal Astronomical Society* 70 (1982) 141–154.
- [20] G. Kletetschka, P.J. Wasilewski, P.T. Taylor, Unique thermoremanent magnetization of multidomain sized hematite: Implications for magnetic anomalies, *Earth and Planetary Science Letters* 176 (3–4) (2000) 469–479.
- [21] G. Kletetschka, P.J. Wasilewski, P.T. Taylor, Hematite vs. magnetite as the signature for planetary magnetic anomalies? *Physics of the Earth and Planetary Interiors* 119 (3–4) (2000) 259–267.
- [22] G. Kletetschka, P.J. Wasilewski, Grain size limit for SD hematite, *Physics of the Earth and Planetary Interiors* 129 (1–2) (2002) 173–179.
- [23] D.J. Dunlop, K.S. Argyle, Thermoremanence, anhysteretic remanence and susceptibility of submicron magnetites: non-linear field dependence and variation with grain size, *Journal of Geophysical Research, [Solid Earth]* 102 (B9) (1997) 20199–20210.
- [24] M.J. Dekkers, Magnetic properties of natural pyrrhotite: II. High- and low-temperature behavior of J_{rs} and TRM as a function of grain size, *Physics of the Earth and Planetary Interiors* 57 (1989) 266–283.
- [25] D.J. Dunlop, Ö. Özdemir, *Rock Magnetism: Fundamentals and Frontiers*, Cambridge University Press, Cambridge, 1997, 573 pp.
- [26] D.J. Dunlop, *Developments in rock magnetism, Reports on Progress in Physics* 53 (1990) 707–792.
- [27] G.J. Borradaile, An 1800-year archeological experiment in remagnetization, *Geophysical Research Letters* 23 (13) (1996) 1585–1588.
- [28] F. Heller, H. Markert, Age of viscous remanent magnetization of Hadrians Wall (Northern-England), *Geophysical Journal of the Royal Astronomical Society* 31 (4) (1973) 395–406.
- [29] Y. Syono, Y. Ishikawa, Magnetostriction constants of $x\text{Fe}_2\text{TiO}_4 \cdot (1-x)\text{Fe}_3\text{O}_4$, *Journal of the Physical Society of Japan* 18 (1963) 1231–1232.
- [30] B.M. Moskowitz, High-temperature magnetostriction of magnetite and titanomagnetites, *Journal of Geophysical Research* 98 (1993) 359–371.
- [31] Y. Syono, Y. Ishikawa, Magnetocrystalline anisotropy of $x\text{Fe}_2\text{TiO}_4 \cdot (1-x)\text{Fe}_3\text{O}_4$, *Journal of the Physical Society of Japan* 18 (1963) 1230–1231.
- [32] E.J. Fletcher, W. O'Reilly, Contribution of Fe^{2+} ions to the magnetocrystalline anisotropy constant K_1 of $\text{Fe}_{3-x}\text{Ti}_x\text{O}_4$ ($0 < x < 0.1$), *Journal of Physics C7* (1974) 171–178.
- [33] M.H. Acuña, J.E.P. Connerney, N.F. Ness, R.P. Lin, D. Mitchell, C.W. Carlson, J. McFadden, K.A. Anderson, H. Rème, C. Mazelle, D. Vignes, P. Wasilewski, P. Cloutier, Global distribution of crustal magnetization discovered by the Mars Global Surveyor MAG/ER Experiment, *Science* 284 (1999) 790–793.
- [34] D. Dunlop, G. West, An experimental evaluation of single-domain theories, *Reviews of Geophysics* 7 (1969) 709–757.